

Stimulated Raman Scattering Mechanisms and Scaling Behavior in Planar Direct-Drive Experiments at the National Ignition Facility

M. J. Rosenberg,¹ A. A. Solodov,¹ W. Seka,¹ R. K. Follett,¹ J. F. Myatt,² A. V. Maximov,¹ C. Ren,³ S. Cao,³ P. Michel,⁴ M. Hohenberger,⁴ J. P. Palastro,¹ C. Goyon,⁴ T. Chapman,⁴ J. E. Ralph,⁴ J. D. Moody,⁴ R. H. H. Scott,⁵ K. Glize,⁵ and S. P. Regan¹

¹Laboratory for Laser Energetics, University of Rochester

²Department of Electrical and Computer Engineering, University of Alberta

³Department of Mechanical Engineering, University of Rochester

⁴Lawrence Livermore National Laboratory

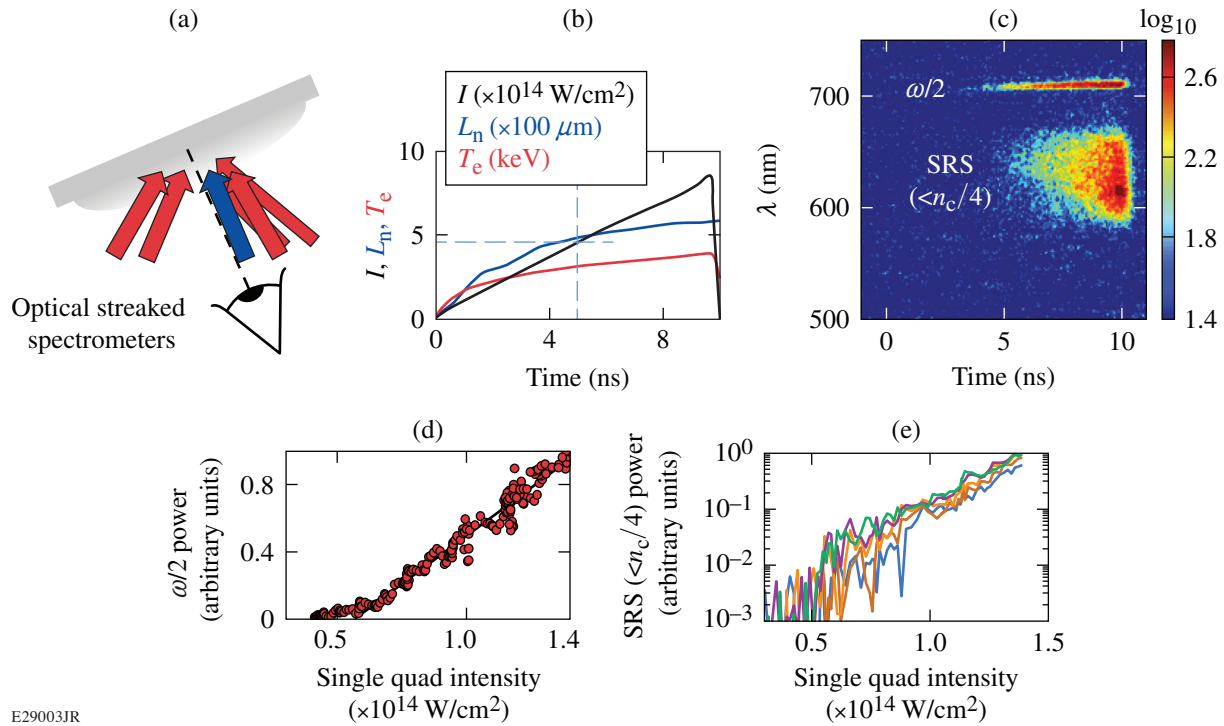
⁵Central Laser Facility, STFC Rutherford Appleton Laboratory

Direct-drive inertial confinement fusion implosions may be susceptible to preheat by hot electrons generated by laser–plasma instabilities. Stimulated Raman scattering (SRS), which occurs at densities around and below the quarter-critical density of the laser [$n_e = n_c/4$, where n_e is the electron density and n_c is the critical density for the laser wavelength λ_0 (in μm), with $n_c \approx 1.1 \times 10^{21} \lambda_0^{-2} \text{cm}^{-3}$], has been observed to be a prominent hot-electron–generating instability in direct-drive experiments at the National Ignition Facility (NIF).¹

Planar-geometry experiments were conducted on the NIF to elucidate the SRS mechanisms present in direct-drive ignition-scale plasmas, intensity thresholds for SRS, and the scaling of SRS with laser intensity for different laser beam angles of incidence. These experiments were designed to achieve plasma conditions relevant to direct-drive–ignition designs, with density scale lengths $L_n \sim 600 \mu\text{m}$, electron temperatures $T_e \sim 4.5 \text{ keV}$, and laser intensities at $n_c/4$ between $I_{n_c/4} \sim 4 \times 10^{14}$ and $1.3 \times 10^{15} \text{ W/cm}^2$.

Figure 1 shows the experimental setup, simulated quarter-critical plasma conditions by the 2-D radiation-hydrodynamic code *DRACO*, and time-resolved SRS spectral data collected along the target normal. As shown in Fig. 1(a), the experiment used 32 beams (eight “quads”) at incidence angles $< 35^\circ$ on a CH ablator and a linearly ramped laser pulse to reach simulated conditions at $n_c/4$ of up to $I_{n_c/4} \sim 8.5 \times 10^{14} \text{ W/cm}^2$, $L_n \sim 580 \mu\text{m}$, and $T_e \sim 4.0 \text{ keV}$ [Fig. 1(b)]. The scattered-light spectrum [Fig. 1(c)] shows two features: a narrow feature at around 710 nm corresponding to half-harmonic ($\omega_0/2$) emission and a broader feature between 600 and 660 nm. The $\omega_0/2$ feature corresponds to an absolute SRS instability at $n_c/4$, while the lower-wavelength feature is generated by SRS in the underdense ($< n_c/4$) region.¹ Lineouts of each feature reveal differences in the time histories of the underlying instabilities. While the $\omega_0/2$ feature increases nearly linearly with laser intensity [Fig. 1(d)], signifying a saturated absolute SRS instability, the underdense SRS feature increases exponentially with laser intensity [Fig. 1(e)], suggesting that this instability is observed in its linear convective stage.

Additional experiments were conducted with the planar target oriented normal to the NIF polar axis. In these experiments, the target was irradiated in cylindrical symmetry by laser beams at well-defined angles of incidence, either 23° and 30° (“inner beams”) or 45° and 50° (“outer beams”). SRS was diagnosed by optical streaked spectrometers at viewing angles of 23° and 50° , revealing different SRS mechanisms, all from the underdense region. As previously observed,¹ SRS was detected at each viewing angle for each of the inner-beam and outer-beam laser drives. The observations at 50° , whether generated by inner or outer beams, are interpreted as tangential sidescatter, with the SRS-scattered light propagating parallel to density contours before refracting and propagating out of the plasma.² The observations at 23° correspond to either backscattered or sidescattered SRS light.



E29003JR

Figure 1

(a) Experimental geometry and SRS observations along the target normal using a ramped laser pulse. The (b) simulated total overlapped laser intensity (black line), density scale length (blue line), and electron temperature (red line) at $n_c/4$ increased continuously with time, corresponding to (c) the time-resolved optical spectrum. The power in each spectral component [(d) $\omega/2$ and (e) sub- $n_c/4$ SRS, with the various colored lines representing the signal integrated over different 5-nm-wide wavelength bands] as a function of the single-quad intensity at $n_c/4$ shows scaling behavior and intensity thresholds.

Within this configuration, several experiments were conducted in which particular “quads” (groupings of four NIF beams) were toggled on or off to elucidate single-quad or multi-quad contributions to the SRS signal. A strong correlation was observed between quads at 50° and the SRS observation at that location, strongly indicating a single-quad tangential sidescatter of outer beams. A moderate correlation was observed between quads at 23° and SRS observations at 50° along the same azimuthal angle, while a stronger correlation was observed between two neighboring inner quads and the 50° SRS measurement. The latter may indicate a multiple-quad effect.³ Other SRS observations at 23° , as well as along the target normal, did not show strong single-quad contributions and therefore are inferred to be generated by many beams.

Notably, in addition to the underdense SRS observed along target normal, the underdense SRS at other viewing locations, corresponding to sidescatter as well as backscatter, all appear to have a near-exponential dependence on laser intensity in experiments with a linear-ramp laser pulse.

Hard x-ray (HXR) measurements were also obtained in order to relate the SRS observations to hot-electron production. Figure 2 shows HXR and SRS data obtained on experiments with either linear-ramp laser pulses or flattop laser pulses driven by inner beams [Fig. 2(c)]. The linear-ramp pulse experiments show a correlation of time-resolved HXR signal and SRS signal from several viewing locations representing scattered light from the underdense region [Fig. 2(a)]. The HXR emission scales nearly exponentially with time—or with laser intensity—on ramp-pulse experiments [Figs. 2(a) and 2(b)], similar to what was observed for the underdense SRS-scattered light as shown in Fig. 1(e) and at other viewing angles. In addition, a time-integrated SRS signal

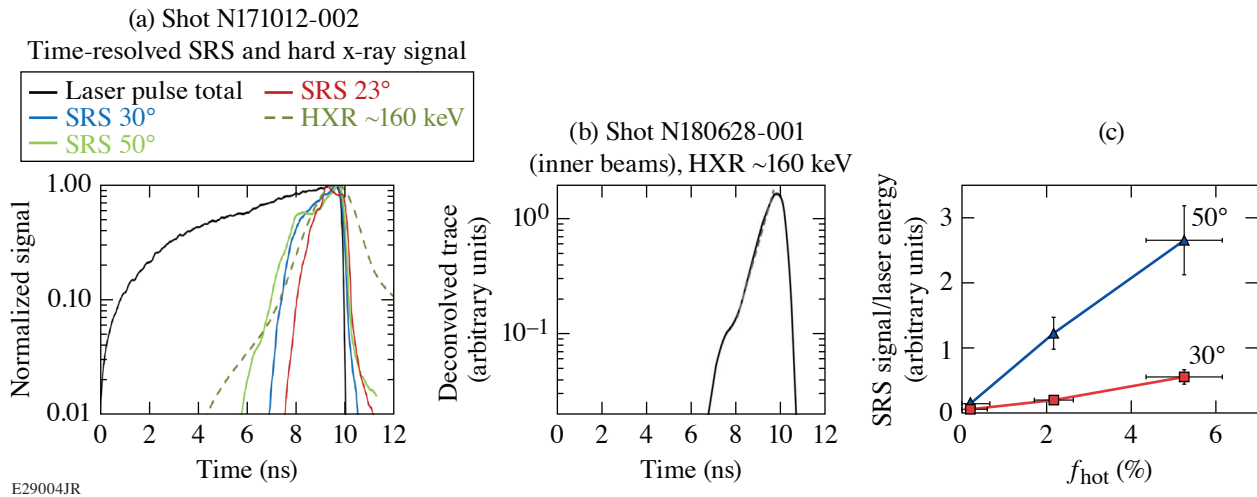


Figure 2

SRS and HXR data from [(a),(b)] ramp pulse and (c) flat-top-pulse experiments driven by inner beams. (a) The normalized time-resolved SRS signals from various viewing angles have a time history similar to 160-keV HXR's. (b) Another ramp-pulse experiment produced a HXR signal that is nearly exponential with time (or with laser intensity). (c) Time-integrated SRS signals at 50° and 30° viewing angles, representing SRS from the underdense region, are directly proportional to the fraction of laser energy converted to hot electrons, indicating a correlation.

measured at 30° and 50° from target normal is directly proportional to the measured fraction of laser energy converted to hot electrons (f_{hot}) [Fig. 2(c)]. The correlation of HXR measurements and these SRS observations suggests a connection between SRS in the underdense region and hot-electron production.

Although further modeling is needed to explain the precise SRS mechanism by which hot electrons are generated, these results can be used to guide direct-drive-ignition designs in which hot-electron preheat coupled to the inner layer of the imploding target must be kept below $\sim 0.1\%$.

This material is based upon work supported by the Department of Energy National Nuclear Security Administration under Award Number DE-NA0003856, the University of Rochester, and the New York State Energy Research and Development Authority.

1. M. J. Rosenberg *et al.*, Phys. Rev. Lett. **120**, 055001 (2018).
2. P. Michel *et al.*, Phys. Rev. E **99**, 033203 (2019).
3. S. Depierreux *et al.*, Phys. Rev. Lett. **117**, 235002 (2016).